

Signature of Baryon Oscillation in the Distribution of Galaxies

Sarah Hansen

1. Introduction

Cosmological parameters governing the matter, dark energy and curvature content of the universe may be investigated by examining the distribution of matter in the universe. The Cosmic Microwave Background (CMB) preserves a record of the matter distribution at the time radiation and matter decoupled; the correlation function of galaxies in the local universe shows how the matter distribution has been recorded by baryons to the present day. Since galaxies form in regions of the universe that are over-dense as a result of the conditions at decoupling, the distribution revealed by the correlation function ought to show similar features as those found in the CMB, albeit modified by the process of gravitational collapse.

While the information in the radiation field has been studied for over a decade, only recently has the galaxy distribution revealed the predicted signatures of being set in place at the the era of recombination. In particular, the correlation function of galaxies is predicted to be generally smooth and falling toward greater separations, but with a bump at separations of approximately $100h^{-1}$ Mpc due to the scale of the sound horizon at recombination. In “Detection of the Baryon Acoustic Peak in the Large-Scale Correlation Function of SDSS Luminous Red Galaxies,” Eisenstein et al. (2005) demonstrate the detection of recombination-epoch acoustic oscillations as imprinted in the distribution of matter in the low-redshift universe. In this paper, we review the cause of the galaxy correlation function baryon peak and summarize the detection and cosmological power of this feature.

2. Formation of the Acoustic Peak

At inflation, the universe contained an almost, but not quite, smooth distribution of matter and radiation. The initial quantum fluctuations caused this slight unevenness to be (almost) scale-independent: that is, there were over- and under-dense regions of every size and with a roughly equal amount of power at each scale. Dark matter, as it can only interact gravitationally, began accreting in the initially slightly over-dense regions. However, as the baryonic matter was all ionized at these times, the baryons and radiation were tightly coupled

via Compton scattering.¹ The tendency of baryons to move deeper into the potential wells of the over-dense regions was resisted by the photon pressure of the radiation. The interplay between gravity and pressure caused the baryon-photon fluid to oscillate acoustically as the matter and radiation moved together in response to the pressure gradients in the plasma.

Each initial peak in the density field was thus an initially over-pressurized region, causing a spherical density wave of coupled photons and baryons to be driven outward from each perturbation at the speed of sound, $c_s = 1/\sqrt{3(1+R)}$, where

$$R(a) = \frac{3}{4} \frac{\rho_b}{\rho_\gamma} \Big|_a = 0.729 \left(\frac{\Omega_b h^2}{0.024} \right) \left(\frac{a}{10^{-3}} \right) T_{rat}^{-4}, \quad (1)$$

is the photon-to-baryon ratio as a function of scale factor and $T_{rat} = T_{CMB}/2.725\text{K}$ (Hu 2004). The outward expansion of the photon-baryon waves from all the initially over-dense regions caused a pattern of over- and under-dense regions in addition to that set by the position of the initial perturbations. This pattern has a characteristic scale corresponding to the distance that the coupled photons and baryons have been displaced from the initial perturbation. This distance is equal to the sound horizon size.

As time progressed and the universe cooled, the sound speed dropped and the propagation of the photon-baryon wave slowed. In addition, photons slowly diffused out of the baryon-photon wave, broadening the pressure wave somewhat. As a result, the oscillation fluctuations on scales smaller than the width of the pressure wave were smoothed out. This effect is known as Silk damping. Meanwhile, the dark matter continued to collect due to gravitation, mainly around the initial perturbations' positions, although with slight displacements due to suffering the gravitational pull of the oscillating baryons and photons.

Eventually, the temperature cooled sufficiently that the optical depth to scattering dropped rapidly, causing the photons to begin freely streaming and the baryons to combine into neutral hydrogen. The times of last scattering and of recombination coincide because the changes in optical depth happen so quickly, but do not happen at exactly the same moment (Hu & Sugiyama 1996). When the photons scatter for the last time, the baryon-photon wave that originated around a particular initial over-density had traveled a distance s_* , the sound horizon at the last scattering epoch, given by

$$s_* = \int_0^{a_*} \frac{da}{a^2 H(a)} c_s(a) = \frac{2\sqrt{3}}{3} \sqrt{\frac{a_*}{R_* \Omega_m H_0^2}} \ln \left(\frac{\sqrt{1+R_*} + \sqrt{R_* + r_* R_*}}{1 + \sqrt{r_* R_*}} \right) \quad (2)$$

¹Neutrinos were not coupled in this way, and, as they were relativistic, they were able to stream away from the initial perturbations. This behavior served to very slightly modify the shape of the baryon-photon wave.

where r_* is the radiation-to-matter ratio, ρ_r/ρ_m , at last scattering (Hu 2004) and R_* is the photon-to-baryon ratio at last scattering. For values of parameters near the concordance cosmology, this size scale scales with the baryon and total matter content of the universe and the fine structure constant as

$$\frac{s_*}{Mpc} \sim 144.4 \left(\frac{\alpha}{\alpha_0}\right)^{-1.36} \left(\frac{\Omega_m h^2}{0.14}\right)^{-0.252} \left(\frac{\Omega_b h^2}{0.024}\right)^{-0.083} \quad (3)$$

The last-scattered photons are imprinted with this characteristic size scale, as the pattern of over- and under-dense regions of matter is preserved as slight temperature variations of the radiation field. The correlation at separations equal to the physical scale of the sound horizon at last scattering is expressed as the now familiar harmonic series of maxima and minima in the power spectrum of the CMB temperature anisotropies.

When the photons decouple from the baryons, the baryons continue to coast, but as peculiar velocities are damped in an expanding universe, within an expansion time the baryons have settled into a stable (in comoving coordinates) density distribution (Hu & Sugiyama 1996). This movement of baryons after the time of decoupling (termed “velocity overshoot”) causes a phase shift of roughly $\pi/2$ with respect to the CMB fluctuations between the two distributions’ power spectra.

After decoupling, the matter perturbations in both dark matter at the initial locations and in baryons that have been carried out to a spherical shell, grow gravitationally. At much later times, these perturbations are the sites of galaxy formation. The central dark matter over-densities dominate the density field compared to the overlapping spherical shells of baryons, and thus galaxies are most likely to form within the central peaks. However, the acoustic feature in the density distribution also gives rise to galaxies. The excess of galaxies at separations corresponding to the distance between the central density peak and the scale of the baryon-photon oscillation at decoupling results in a feature in the matter correlation function. This location of this feature in the correlation function is at ~ 150 Mpc (comoving) (Eisenstein et al. 2005).

Traditionally, the CMB anisotropies have been studied via their power spectrum, the Fourier transform of the correlation function. Doing the analysis in frequency space rather than configuration space is preferred for the CMB because power in different Fourier modes is statistically independent for standard cosmologies. However, for investigating the distribution of matter in the local universe, the correlation function offers crucial advantages. The independence of Fourier modes becomes difficult to ensure on large scales for surveys with complicated geometry such as that of the SDSS (although the SDSS data are largely contiguous, the boundaries are ragged compared to the scales of interest). The information

required to make accurate computations lies in the off-diagonal elements of the covariance matrix of the correlation function, which may be computed. Additionally, the effects of small-scale deviations due to non-linear structure formation, gas physics within halos, and shot noise do not mix into large scales in the correlations function, so these issues do not plague the measurement of the larger-scale acoustic peak position.

3. Using the Correlation Function for Cosmology

3.1. The Acoustic Peak

The existence, strength, and scale of the signature in the galaxy correlation function of acoustic oscillations in the early universe are all sensitive to the underlying cosmology of our universe. First, the existence of such a feature offers exciting confirmation in the local universe that the interpretation of the $z \sim 1000$ CMB fluctuations as an acoustic phenomenon is valid, and that the notion of linear large-scale structure growth due to gravitational clustering is well-founded. In addition, the amplitude of the acoustic feature relative to the overall normalization of the galaxy correlation function is quite sensitive to the baryon fraction $f_B = \Omega_{B0}/\Omega_{M0}$ (Matsubara 2004) and thus the existence but low-contrast of the feature is evidence for dark matter at the era of recombination. Furthermore, the narrowness of the peak in physical units allows for the peak scale to be used as a standard ruler: the size of the peak may be measured locally and compared to the size predicted from the physics of the primordial plasma, thus constraining the cosmology-dependent distance to the galaxy sample (Eisenstein et al. 2005).

Using the acoustic peak in the galaxy correlation function as a standard ruler offers the most stringent constraints on cosmology with these data. The characteristic separation is dependent on the expansion history of the early universe and the sound speed in the plasma, and scales as $\Omega_m h^2$ and $\Omega_b h^2$ (Eq. 3). These two quantities are well constrained by the CMB power spectrum alone, and so may be confidently used to predict the expected scale of the acoustic peak in the galaxy correlation function. The comparison of the CMB acoustic peak scale and the galaxy correlation function scale constrains H_0 , and thus Ω_m , independent of the angular diameter distance to last scattering (Eisenstein et al. 1998). Given a distance to the galaxies, the observed angular scale of the acoustic signal can be converted into a physical scale. That physical scale must be equal to that given by the CMB physics. Thus, the best-fit cosmological parameters are those used to determine the distance that makes the angular acoustic scale correspond to a physical scale of 150 Mpc.

This distance determination has uncertainty due to the uncertainty of the observables

used to produce the galaxy correlation function, but also due to the uncertainty in measuring the angular extent of the CMB patches. That is, since (in frequency space) $l = k_s D_A$, where k_s is the angular scale of the sound horizon, $k_s = 2\pi/s_*$, the measurement of any given frequency mode l has uncertainty from both the sound horizon estimate and the angular diameter distance D_A to the redshift in question. However, by measuring the ratio of the distance to the mean galaxy redshift to the distance to the last scattering epoch, the factor of k_A cancels, removing the uncertainty due to $\Omega_m h^2$ and other uncertainties such as the possibility of additional relativistic species causing a different sound horizon size. The resulting distance ratio is therefore a more robust distance measurement than just the distance to the galaxies alone.

3.2. The Correlation Function Shape

The shape of the correlation function contains information about several cosmological quantities: $\Omega_m h^2$, $\Omega_b h^2$, spectral tilt of the initial perturbations n , and the neutrino mass. As discussed above, the first two govern the position of the acoustic peak, while the latter two both tilt the low-redshift power spectrum without affecting the position of the acoustic signature. Silk damping and non-linear gravity models broaden the acoustic feature. Thus, given a set of cosmological parameters, the correlation function shape may be predicted from linear theory.

The details of non-linearity are important, however, for the precision measurements possible with these data. Results from N-body and semi-analytic halo modeling are included to account for effects of non-linear gravity, redshift distortions, mode coupling, non-linear collapse, and halo bias. These corrections are small (within 1% for scales greater than $30h-1$ Mpc, (Eisenstein et al. 2005, Fig. 5)), and are unable to masquerade as a false large-scale correlation.

4. The LRG Sample and Determination of the LRG Correlation Function

The set of galaxies used for this study is the Luminous Red Galaxy (LRG) sample of the Sloan Digital Sky Survey (SDSS). These galaxies are selected from the SDSS imaging survey to be intrinsically luminous, red galaxies; they are then targeted for spectroscopy in the SDSS spectroscopic survey. The details of selecting these galaxies are given in Eisenstein et al. (2001), but are summarized here.

The LRG sample was designed to contain a volume-limited set of red, $L \geq 3L_*$ galaxies

to $z \sim 0.5$; such a sample is useful for studies of large-scale structure, testing the predictions of hierarchical galaxy formation, and for providing spectroscopic redshifts for clusters selected from SDSS imaging data. The SDSS combines an imaging survey in u, g, r, i , and z of the northern Galactic cap and an extensive spectroscopic follow-up program. Cuts are made on r magnitude and $g - r$ and $r - i$ colors to select galaxies that are likely to be early-types to $z \sim 0.5$. The LRG sample comprises 46,748 galaxies distributed in the redshift range $0.16 < z < 0.47$ over 3816 square degrees, or $0.72h^{-3}\text{Gpc}^3$ (Eisenstein et al. 2005). The typical redshift of the sample is $z = 0.35$. At this distance, the 150 Mpc acoustic scale is approximately 6 degrees.

The correlation function of LRGs, $\xi(s)$, is measured by comparing the distribution of comoving separation between each pair of galaxies in the LRG sample to the distribution for galaxy-random point pairs. The excess clustering of LRG-LRG pairs over random is the correlation function. To make this measurement, a cosmology must be assumed for calculating the comoving distance between galaxies with observed positions in (ra, dec, z) space. The comoving distance, s , depends on cosmological parameters according to:

$$s = \int_a^1 \frac{da}{a^2 H(a)} = \frac{1}{H_0} \int_a^1 (\Omega_{m,0} \cdot a + \Omega_{r,0} + \Omega_{\Lambda,0} \cdot a^4 + \Omega_{\kappa,0} \cdot a^2)^{-1/2} da. \quad (4)$$

The fiducial cosmology assumed is flat, $\Omega_m = 0.3$, $\Omega_\Lambda = 0.7$, although these parameters are later included in the parameter estimation. The resulting measurement of the correlation function of LRGs is in Figure 1 (Eisenstein et al. 2005, Fig. 2).

The uncertainties in the data and on the cosmological parameters are measured using the full covariance matrix, determined from a combination of mock catalog studies and jackknife estimation. [Due primarily to the large scales being studied, it is infeasible to use only jackknife error estimation because the data does not support the number of samples required to ensure a stable result.] Using the fiducial cosmology, the authors generate 1278 mock catalogs with a halo model that includes redshift distortions, second-order clustering, and small-scale halo structure. Each catalog has independent initial conditions; the scatter in results among the correlation functions determined from the set of mocks allows for characterization of the covariance matrix. Additionally, the SDSS survey region is divided into ten non-overlapping jackknife regions; the covariance matrix recovered from this method is comparable to that determined from the mocks. For uncertainties in the derived cosmological parameter values, the mock catalog covariance is used to find the best-fit parameters for each of the 10 jackknife samples, and the uncertainty for each parameter is taken to be the rms scatter between the values estimated in the set of jackknife samples.

There are several opportunities for systematic error and/or bias in the LRG sample and correlation function determination, each of which the authors handle carefully. The LRG selection is highly sensitive to uncertainty in photometry in g, r , and i bands, but due to the precision of the SDSS imaging camera and the accuracy of the photometric calibration, these bands have $\leq 1\%$ scatter, which translates to scatter of 0.02 in $\xi(s)$. However, due to the survey strategy of the SDSS, long, narrow strips of sky are calibrated at once, resulting in about 20 independent calibrations being applied to a circular region with a radius equal to the scale of the acoustic peak. In addition, as calibration errors could only produce large scale correlation along the length of each strip of data (*i.e.* along the scan direction of the survey), such systematics would be unable to produce the narrow feature observed in the correlation function. Hence, the systematic error in $\xi(s)$ due to calibration must be less than 0.01 (Eisenstein et al. 2005).

The correlation function is susceptible to bias if redshift distortions and clustering bias of LRGs are not properly included. The former has the effect of making a given large-separation correlation smaller along the line of sight than along the tangential direction, and is managed via measuring a spherically averaged correlation function over four bins in angular separation from the line of sight. The clustering bias is parametrized as a function of redshift, and as such varies by less than 0.5% as a function of scale. Hence, the systematic bias caused by a correlation of scale with redshift is negligible (Eisenstein et al. 2005).

5. Cosmology from the LRG Correlation Function

5.1. Distance and $\Omega_m h^2$

In principle, the measured acoustic peak scale can be used to constrain cosmology via the distance to the LRG sample. For obtaining the correlation function over a grid of cosmological parameters, however, it is far computationally simpler to apply a scale dilation to the distance, rather than recomputing the correlation function every time. However, the question arises: which distance? The typical redshift of the LRG sample is $z = 0.35$, but the galaxies are distributed in a range of redshifts around this middle value.

In practice, measuring the distance to the LRG sample using the acoustic peak as a standard ruler is complicated by two issues related to the extent of the spatial distribution of the galaxies. First, using a different set of values for the cosmological parameters wrapped up in determining the separations between galaxies introduces a redshift-dependent change in the distances. However, this effect is small: a 3% change in distance across the redshifts of the LRG sample for Ω_m between 0.2 and 0.3. Second, the Hubble parameter changes

differently than the angular diameter distance, and thus the separations measured are some combination of the line-of-sight and transverse distances. This combination is modeled by taking the equivalent distance measured to redshift z to be expressed in terms of the Hubble distance and the angular diameter distance as

$$D_V(z) = \left[(D_M(z))^2 \frac{cz}{H(z)} \right]^{1/3}. \quad (5)$$

$H(z)$ is the Hubble parameter and $D_M(z)$ is the angular diameter distance:

$$D_M(z) = \frac{1}{1+z} \frac{H_0^{-1}}{\sqrt{|\Omega_{\kappa,0}|}} S_{\kappa} \left[\sqrt{|\Omega_{\kappa,0}|} \int_0^z \frac{dz'}{E(z')} \right] \quad (6)$$

with $E(z) = H(z)/H_0 = [\Omega_m(1+z)^3 + \Omega_{\Lambda}(1+z)^{3+3w_0}]^{1/2}$. Results are given for $D_V(z = 0.35)$, the equivalent distance to the typical LRG redshift.

As discussed in Section 3.1, the ratio of the distance to the LRGs to the distance to the CMB is particularly robust. Eisenstein et al. (2005) denote this ratio as

$$R_{0.35} = \frac{D_V(0.35)}{D_M(1089)}, \quad (7)$$

where $D_M(1089)$ is the angular diameter distance to the epoch of last scattering (as the CMB measures purely a transverse distance).

Cosmological parameter estimation is done by computing χ^2 from the covariance matrix for a range of cosmological models that vary $\Omega_m h^2$ and $D_V(0.35)$. $\Omega_b h^2$ and n are held fixed at 0.024 and 0.98 respectively, as they are well-constrained from WMAP, Lyman- α forest, and big bang nucleosynthesis studies. The curves plotted in Figure 1 are for values of $\Omega_m h^2 = 0.12$ (top, green), 0.13 (red), and 0.14 (bottom with peak, blue). The bottommost, magenta line shows the model for pure CDM, which has no acoustic peak. Comparing the best-fit model ($\Omega_m h^2 = 0.13$) with the no-acoustic peak prediction of CDM, the acoustic peak is detected at 3.4σ significance. Figure 2 shows the $\Omega_m h^2 - D_V(0.35)$ constraints from Eisenstein et al. (2005, Fig. 7). The Figure gives the χ^2 contours for 1σ to 5σ for a 2D Gaussian likelihood. The distance $D_V(0.35)$ is constrained to 4.7%, a remarkably tight uncertainty for an astronomical distance. The relative distance measure, $R_{0.35}$ is constrained to 3.7%.

To test the result, the authors repeat the measurement with all but the two smallest separation bins in the correlation function; with a varying perturbation spectrum tilt; with a changing baryon density; and by removing the corrections for non-linear gravity, and scale-dependent bias and redshift distortions. In all cases, the determined cosmological parameters change somewhat, but the constraint on $R_{0.35}$ remains unchanged.

5.2. Dark Energy and Spatial Curvature

The correlation function of LRGs in combination with CMB data can be used to place constraints on simple models of the dark energy and spatial curvature. For a flat model, the data can constrain values of w if w is constant. Or, for an assumed $w = -1$, the data constrain the amount of curvature. These constraints are most easily seen by plotting the likelihood contours for $\Omega_m h^2 - D_V(0.35)$ and overlaying curves corresponding to the model predictions from a grid of constant w or constant curvature values.

The flat model only gives a w to within ~ 0.2 , as Ω_m is not yet sufficiently well known to allow a better determination (Eisenstein et al. 2005, Fig. 10a). However, for the $w = -1$ model, the curvature is constrained to 1%, largely because the distance to the last scattering surface is so sensitive to curvature (Eisenstein et al. 2005, Fig. 12a). A more general model with a redshift-dependent $w(z)$ requires additional information to break the parameter degeneracies; a detection of the acoustic peak signature in the correlation function of a higher-redshift sample of galaxies would be one way to provide another constraint.

The distance ratio $R_{0.35}$ is consistent with a cosmological constant cosmology. In a cosmological model without dark energy, a curvature of $\Omega_\kappa = 0.30$ is required to match the distance ratio observed. Such a curvature is entirely inconsistent with results from the CMB power spectrum, the cluster baryon fraction, and the observed value of H_0 . With a prior that the universe is flat, the LRG data give evidence for the existence of dark energy.

6. Conclusions

This paper (Eisenstein et al. 2005) documents the first significant detection of the signature of early universe acoustic oscillations in the distribution of galaxies in the local universe. By measuring the correlation function of luminous red galaxies in the Sloan Digital Sky Survey, the “baryon wiggle” in the correlation function at $\sim 100h^{-1}$ Mpc is identified at greater than 3σ . This detection was made possible by having, for the first time, nearly $1h^{-3}$ Gpc³ of survey volume available for study.

The detection confirms three basic tenets of CDM cosmological theory. First, the existence of the peak, a feature that is unable to be inflicted upon the correlation function by some conspiracy of systematic bias or uncertainty, is a confirmation that the primordial plasma acoustically oscillated, producing the pattern of temperature anisotropies recorded in the CMB. Second, the small amplitude of the peak demonstrates the existence of matter that does not interact with the photon-baryon fluid except gravitationally. That is, the peak amplitude provides evidence for dark matter at $z \sim 1100$. Third, that the peak is narrow

indicates that linear collapse dominates the growth of the initial perturbations: non-linear gravitational perturbation theories generically predict that the peak would be much broader, if not washed out entirely, due to coupling of Fourier modes.

The narrowness of the LRG correlation function peak affords the opportunity to measure the distance to the typical LRG redshift. This distance is constrained to better than 5%. In addition, the ratio of the distance to the LRGs to the distance to the surface of last scattering, given by the ratio of the angular scale of the baryon peak to the angular scale of the CMB fluctuations, is well constrained to better than 4% and robust to vagaries of analysis (*e.g.* choice of angular separation bins used in fitting) and cosmology (*e.g.* choice of n). The distance ratio is consistent with a cosmological constant cosmology, and although tight constraints are not achievable with these data, with the assumption of a flat universe, the LRG correlation function provides geometric evidence for dark energy.

To improve cosmological constraints, additional data are needed. If additional, higher redshift survey volumes of order $1h^{-3} \text{ Gpc}^3$ can be examined, the acoustic scale can be measured over a range of redshifts, and used to greatly improve the determination of $w(z)$ and spatial curvature. The next generation of galaxy surveys may be able to offer such promising data.

REFERENCES

Eisenstein, D. J., Hu, W., & Tegmark, M. 1998, ApJ, 504, L57

Eisenstein, D. J., et al. 2001, AJ, 122, 2267

Eisenstein, D. J., et al. 2005, ApJ, 633, 560

Hu, W. 2004, astro-ph/0407158

Hu, W., & Sugiyama, N. 1996, ApJ, 471, 542

Matsubara, T. 2004, ApJ, 615, 573

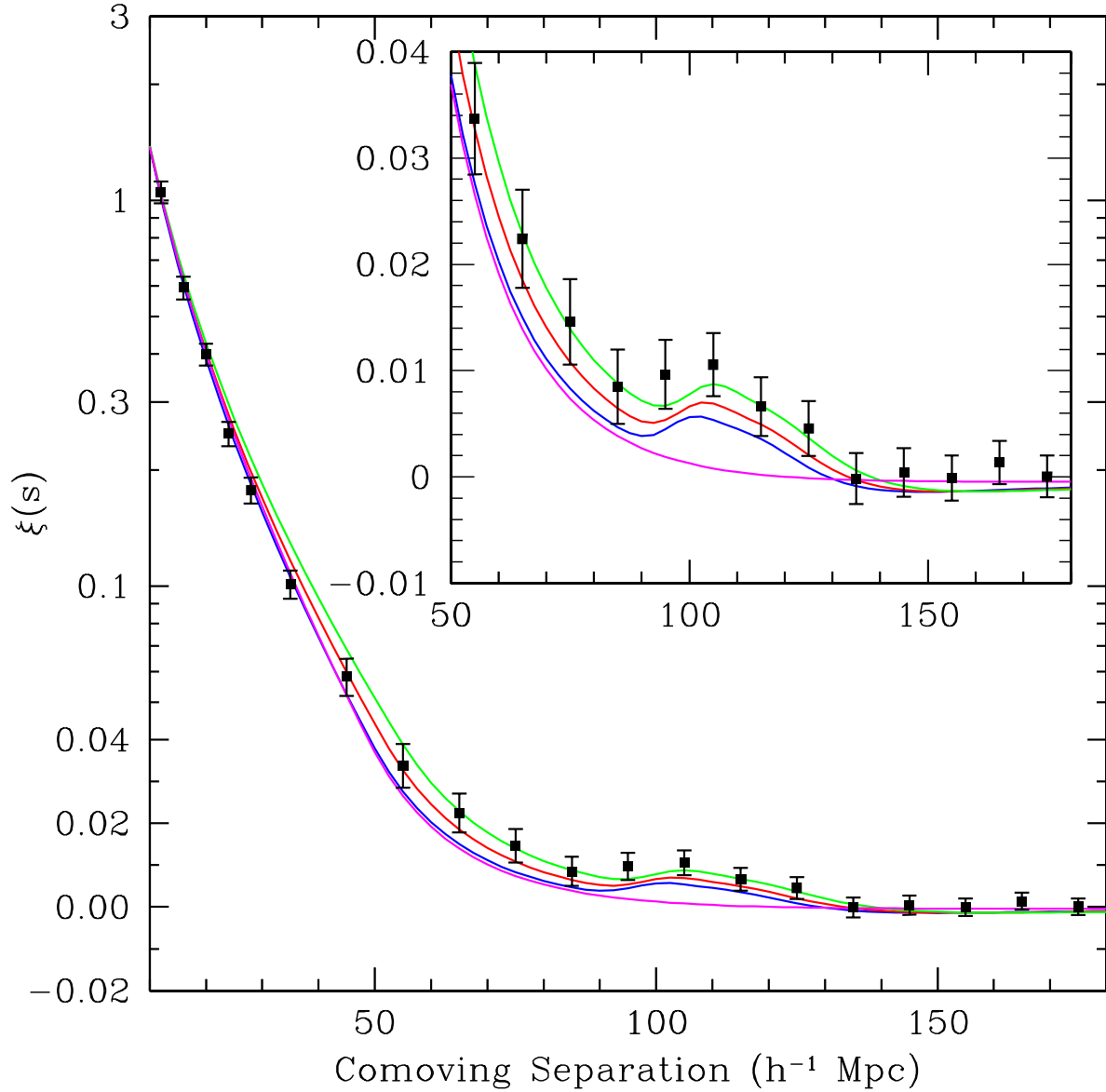


Fig. 1.— The correlation function of the SDSS LRG sample. Note that the error bars reflect the diagonal elements of the covariance matrix from the mock catalog, but the data are correlated. The models are $\Omega_m h^2 = 0.12$ (top, green), 0.13 (red), and 0.14 (bottom with peak, blue). The bottommost, magenta line shows the model for pure CDM, with $\Omega_m h^2 = 0.105$. $\Omega_b h^2$ and n are held fixed at 0.024 and 0.98 respectively. The bump at approximately $100h^{-1}$ Mpc is statistically significant. The inset shows the region of interest with a linear vertical axis. (Eisenstein et al. 2005, Fig2)

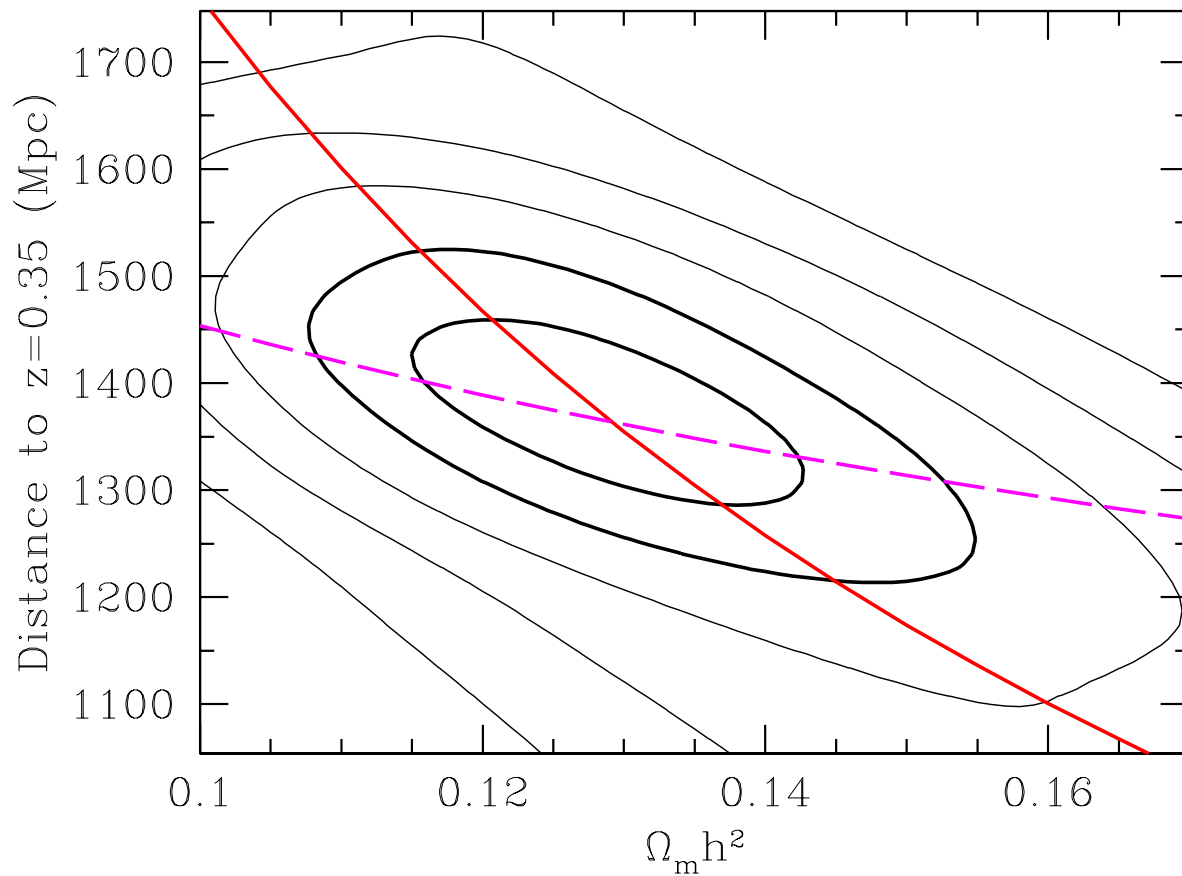


Fig. 2.— Likelihood contours for $\Omega_m h^2$ and $D_V(0.35)$. The contours correspond to 1σ to 5σ for a 2D Gaussian likelihood. The overplotted lines show the two main degeneracy directions: constant $\Omega_m h^2 D_V(0.35)$ (solid, red) and constant sound horizon (dashed, magenta). The former would be the degeneracy direction for a pure CDM model. (Eisenstein et al. 2005, Fig. 7)